ANGULAR RESOLUTION LIMIT OF TWO CLOSELY-SPACED POINT SOURCES BASED ON HYPOTHESIS TESTING

Wei Zhu, Jun Tang and Shuang Wan

Department of Electronic Engineering, Tsinghua University, Beijing, 100084, P. R. China
zhuwei11@mails.tsinghua.edu.cn, {tangj_ee, wanshuang}@mail.tsinghua.edu.cn

ABSTRACT

In this paper, we consider the statistical angular resolution limit (ARL) on resolving two closely-spaced point sources in array processing based on the framework of hypothesis testing. A more general formulation of the linearized hypothesis test is proposed and a new analytical expression of the ARL is derived. The result is more general and its superiority over previous work is verified via numerical simulations. For the first time, we also investigate the case of two identical sources where a second-order approximation is necessary. Numerical simulations show that the theoretical result agrees with the Cramér-Rao bound (CRB) criterion-based ARL with regard to the relation between the resolution limit and the signal-to-noise-ratio (SNR).

Index Terms— angular resolution limit, array processing, hypothesis test, generalized likelihood ratio test, Wald test

1. INTRODUCTION

The ability of resolving two closely-spaced sources is a key performance metric in a variety of applications and has been widely studied in the literature [1–16]. Basically, there are three different types of methods to treat this problem. The first one is based on the null spectrum or the cross-ambiguity spectrum concerning a specific algorithm [5–9]. The second one is based on estimation theory and adopts a Cramér-Rao bound (CRB) based criterion [10,11]. The last one is based on detection theory and uses the hypothesis test formulation [12–15]. It is shown in [14] that a strong relation exists between the angular resolution limits (ARLs) based on the CRB criterion and the hypothesis test formulation.

In a recent work [1], the asymptotic resolvability of two closely-spaced sources in the presence of known subspace interference was investigated using a generalized likelihood ratio test (GLRT) based method. A binary hypothesis test is formulated, in which the hypothesis $\mathcal{H}_1$ embodies the case where two distinct signals are present with parameters ω_1 and ω_2 respectively, and the hypothesis $\mathcal{H}_0$ represents the case where the two sources are unresolvable and merge into a "single" source with a center parameter $\omega_c = \frac{\omega_1+\omega_2}{2}$ (i.e., at the midpoint). However, it should be noted that where the two sources coalesce does not necessarily lie at the midpoint as the two source signals are not necessarily of equal strength. Moreover, the analysis in [1] was based on a first-order approximation of the signal model. The case of two identical sources where higher-order approximation is necessary was not considered, and was believed to be untractable in [4]. In this paper, we consider the derivation of the ARL based on the hypothesis test formulation. The ARL in this context is defined as the minimum angular distance that allows correct determination of the number of sources for pre-specified probabilities of detection and false alarm. For simplicity, we focus on the interference-free case. Our contribution is two-fold: i) A more general form of the hypothesis test is presented and a new criterion, minimum probability of detection (MPD), is proposed in determination of the parameter of interest in $\mathcal{H}_0$. Exploiting these results, a new closed-form expression of the ARL is derived. ii) The special case of two identical sources is considered. We derive an ARL based on a second-order approximation of the signal model.

The remainder of the paper is organized as follows. In section II, we introduce the signal model. In section III-A, we develop the new approach and derive the closed-form expression of the ARL for the general case. In section III-B, we derive the ARL for the special case of two identical sources. In section IV, we present numerical examples for the results derived in Section III. Finally, we draw the conclusion in Section V.

Notation: Throughout this paper, matrices are denoted by bold italic capital letters, and vectors by bold italic lowercase letters. Superscript $(\cdot)^T$ and $(\cdot)^H$ denote transpose and conjugate transpose, respectively. $\|\cdot\|$ denotes the Euclidean norm. $\otimes$ and $\odot$ denote the Kronecker products and Hadamard products, respectively. $\boldsymbol{I}_L$ stands for the $L \times L$ identity matrix. $\mathbb{R}$ and $\mathbb{C}$ denote the set of all real numbers and the set of all complex numbers, respectively. $\Re\{\cdot\}$ denotes the real part of a complex scale. Finally, $(x)^+$ represents $\max(x, 0)$.

This work was supported in part by National Natural Science Foundation of China under Grant 61171120, the Key National Ministry Foundation of China under Grant (9140A07020212JW0101), the Foundation of Tsinghua University under Grant 20101081772, the Foundation of National Laboratory of Information Control Technology for Communication System of China, and the Foundation of National Information Control Laboratory.

2. SIGNAL MODEL

Consider a linear sensor array consisting of N elements with known positions given by the vector $\boldsymbol{d} = [d_1 \;\; d_2 \;\; \cdots \;\; d_N]^T$, $\boldsymbol{d} \in \mathbb{R}^{N\times 1}$. Let $\boldsymbol{s}_1 = [s_1(1) \;\; s_1(2) \;\; \cdots \;\; s_1(L)]^T$ and $\boldsymbol{s}_2 = [s_2(1) \;\; s_2(2) \;\; \cdots \;\; s_2(L)]^T$ denote two far-field and narrow-band source signals in L snapshots, $\boldsymbol{s}_1, \boldsymbol{s}_2 \in \mathbb{C}^{L\times 1}$. The measurement model is

$$\boldsymbol{y}(l) = \boldsymbol{v}(\omega_1)s_1(l) + \boldsymbol{v}(\omega_2)s_2(l) + \boldsymbol{n}(l) \tag{1}$$

where $\boldsymbol{v}(\omega_k)$, $k = 1, 2$ denote the two linearly-independent array steering vectors, $\boldsymbol{v}(\omega_k) = [e^{j\omega_k d_1} \;\; e^{j\omega_k d_2} \;\; \cdots \;\; e^{j\omega_k d_N}]^T$. $\omega_k = \frac{2\pi}{\nu}\cos\theta_k$ is the parameter of interest, with θ_k denoting the direction of arrival relative to the baseline of the array and ν denoting the wavelength. The additive noise vector $\boldsymbol{n}(l)$ is modeled as independent and identically distributed (i.i.d.) circular symmetric complex Gaussian vector with zero-mean and covariance matrix $\sigma^2\boldsymbol{I}_N$, where σ^2 is assumed to be known. We assume that $\sum_{i=0}^{N} d_i = 0$ without loss of generality, as for an arbitrary linear array, we can always specify an origin of coordinate to meet this condition. Furthermore, we assume that the two source signals are deterministic and unknown. Letting $\boldsymbol{z} \triangleq \left[\boldsymbol{y}(1)^T \;\; \boldsymbol{y}(2)^T \;\; \cdots \;\; \boldsymbol{y}(L)^T\right]^T$ and $\boldsymbol{w} \triangleq \left[\boldsymbol{n}(1)^T \;\; \boldsymbol{n}(2)^T \;\; \cdots \;\; \boldsymbol{n}(L)^T\right]^T$, a compact form for the signal model can be written as

$$\boldsymbol{z} = \boldsymbol{V}_1\boldsymbol{s}_1 + \boldsymbol{V}_2\boldsymbol{s}_2 + \boldsymbol{w} \tag{2}$$

where $\boldsymbol{V}_1 = \boldsymbol{I}_L \otimes \boldsymbol{v}(\omega_1)$ and $\boldsymbol{V}_2 = \boldsymbol{I}_L \otimes \boldsymbol{v}(\omega_2)$.

3. THE DERIVATION OF THE ARL

This section is devoted to the derivation of the ARL. In section III-A, a more general form of the hypothesis test formulation is presented and a new closed-form expression of the ARL for the general case is derived, in contrast to [1]. In section III-B, the ARL for the special case of two identical sources is deduced based on a second-order approximation.

3.1. New ARL for the General Case

Let hypothesis $\mathcal{H}_0$ denote the case where the two sources coalesce into a single signal with parameter ω_0, and hypothesis $\mathcal{H}_1$ the case where two signals are present. As with most hypothesis test-based approaches (see e.g., [1] and [12]), we assume that ω_0 is pre-estimated. In contrast to the assumption that $\omega_0 = \omega_c$ in [1] where $\omega_c = \frac{\omega_1+\omega_2}{2}$ is the center parameter, we define $\delta_1 \triangleq \omega_0 - \omega_1$ and $\delta_2 \triangleq \omega_2 - \omega_0$ without any constraint on ω_0. Consequently, the binary hypothesis test formulation for this problem can be given by

$$\begin{cases} \mathcal{H}_0 : (\delta_1, \delta_2) = (0, 0) \\ \mathcal{H}_1 : (\delta_1, \delta_2) \neq (0, 0) \end{cases} \tag{3}$$

where δ_1 and δ_2, viz., ω_1 and ω_2 are unknown to the detector. We take advantage of the fact that δ_1 and δ_2 are small. A first-order approximation of the signal model around $(\delta_1, \delta_2) = (0, 0)$ leads to a linearized (w.r.t. δ_1 and δ_2) form as follows

$$\boldsymbol{z} = \boldsymbol{V}_0\boldsymbol{s}_+ + \dot{\boldsymbol{V}}_0\boldsymbol{s}_- + \boldsymbol{w} \tag{4}$$

where $\boldsymbol{V}_0 = \boldsymbol{I}_L \otimes \boldsymbol{v}(\omega_0)$, $\dot{\boldsymbol{V}}_0 = \frac{\partial \boldsymbol{V}_0}{\partial \omega_0}$, $\boldsymbol{s}_+ = \boldsymbol{s}_1 + \boldsymbol{s}_2$ and $\boldsymbol{s}_- = \delta_2\boldsymbol{s}_2 - \delta_1\boldsymbol{s}_1$. Consequently, the binary hypothesis test can be rewritten as

$$\begin{cases} \mathcal{H}_0 : \boldsymbol{s}_- = \boldsymbol{0},\; \boldsymbol{s}_+ \\ \mathcal{H}_1 : \boldsymbol{s}_- \neq \boldsymbol{0},\; \boldsymbol{s}_+ \end{cases} \tag{5}$$

The GLRT is the most commonly used solution for such a problem. Exploiting the assumption that $\sum_{i=0}^{N} d_i = 0$, we have $\boldsymbol{V}_0^H\dot{\boldsymbol{V}}_0 = \boldsymbol{0}$. The GLRT-based detector is then given by [17]

$$T_G = \frac{\boldsymbol{z}^H\dot{\boldsymbol{V}}_0\left(\dot{\boldsymbol{V}}_0^H\dot{\boldsymbol{V}}_0\right)^{-1}\dot{\boldsymbol{V}}_0^H\boldsymbol{z}}{\sigma^2/2} \underset{\mathcal{H}_0}{\overset{\mathcal{H}_1}{\gtrless}} \eta_1 \tag{6}$$

where η_1 denotes the detection threshold. The detection performance of this detector is characterized by [17]

$$P_f = Q_{\chi^2_{2L}}(\eta_1) \tag{7}$$

$$P_d = Q_{\chi'^2_{2L}(\lambda)}(\eta_1) \tag{8}$$

$$\lambda = \frac{2\|\boldsymbol{d}\|^2}{\sigma^2}\|\delta_2\boldsymbol{s}_2 - \delta_1\boldsymbol{s}_1\|^2 \tag{9}$$

where $Q_{\chi^2_{2L}}$ is the right tail probability for a central chi-squared probability density function (PDF) with $2L$ degrees of freedom, and $Q_{\chi'^2_{2L}(\lambda)}$ is the right tail probability for a noncentral chi-squared PDF with $2L$ degrees of freedom and noncentrality parameter λ.

Recall that ω_0 is assumed to be pre-estimated. To gain further insight, it is more appropriate to assume that the parameter of the single source, ω_0, is asymptotically equal to its maximum likelihood estimate (MLE) when actually two *noise-free* source signals are present. *asymptotic* refers to either $N \to \infty, L \to \infty$ or high signal-to-noise ratio (SNR) value in the array processing context [18]. Under the maximum likelihood estimation, the single source signal most resembles the two source signals and thus the decision is most difficult to make. Therefore, we propose to select the value of ω_0 that minimizes the probability of detection under a pre-specified probability of false alarm instead. This is similar to maximizing the minimum probability of error (MPE) in the Bayesian framework [15]. Let $\delta = \omega_2 - \omega_1$ denote the sources separation. As P_d is a monotonically increasing function of the noncentrality parameter λ, we minimize λ under the constraint $\delta_1 + \delta_2 = \delta$, i.e.,

$$\begin{cases} \underset{\delta_1,\delta_2}{\min} & \lambda \\ \text{s.t.} & \delta_1 + \delta_2 = \delta \\ & \delta_1, \delta_2 \in \mathbb{R} \end{cases} \tag{10}$$

Substituting $\delta_1 = \delta - \delta_2$ into (9) and minimizing λ subject to $\delta_2 \in \mathbb{R}$, it follows that

$$\lambda_{\text{min}} = \frac{2\|\boldsymbol{d}\|^2}{\sigma^2} \frac{\|\boldsymbol{s}_1\|^2\|\boldsymbol{s}_2\|^2 - \Re\{\boldsymbol{s}_1^H \boldsymbol{s}_2\}^2}{\|\boldsymbol{s}_1\|^2 + \|\boldsymbol{s}_2\|^2 + 2\Re\{\boldsymbol{s}_1^H \boldsymbol{s}_2\}} \delta^2 \tag{11}$$

and the optimal ω_0 is given by

$$\hat{\omega}_0 = \omega_c + \frac{|\boldsymbol{s}_2|^2 - |\boldsymbol{s}_1|^2}{2(|\boldsymbol{s}_1|^2 + |\boldsymbol{s}_2|^2 + 2\Re\{\boldsymbol{s}_1^H \boldsymbol{s}_2\})} \delta \tag{12}$$

For pre-specified $P_f = p_f$ and $P_d = p_d$, we can obtain the noncentrality parameter λ by solving the equation $Q^{-1}_{\chi^2_{2L}}(p_f) = Q^{-1}_{\chi'^2_{2L}(\lambda)}(p_d)$, where $Q^{-1}_{\chi^2_{2L}}$ is the inverse of $Q_{\chi^2_{2L}}$ and $Q^{-1}_{\chi'^2_{2L}(\lambda)}$ is the inverse of $Q_{\chi'^2_{2L}(\lambda)}$. Finally, from (11) we obtain the ARL as follows

$$\delta^{(1)}_{\text{lim}} = \sqrt{\frac{\lambda\sigma^2}{2\|\boldsymbol{d}\|^2} \frac{\|\boldsymbol{s}_1\|^2 + \|\boldsymbol{s}_2\|^2 + 2\Re\{\boldsymbol{s}_1^H \boldsymbol{s}_2\}}{\|\boldsymbol{s}_1\|^2\|\boldsymbol{s}_2\|^2 - \Re\{\boldsymbol{s}_1^H \boldsymbol{s}_2\}^2}} \tag{13}$$

The ARL according to [1, eqn. (55)] in the absence of interference is given by

$$\delta^{([1,\text{eqn.}55])}_{\text{lim}} = \sqrt{\frac{2\lambda}{\|\boldsymbol{d}\|^2} \frac{\sigma^2}{\|\boldsymbol{s}_1 - \boldsymbol{s}_2\|^2}} \tag{14}$$

Comparing (13) with (14), it can be seen that the two ARLs are inequivalent unless the two sources are of equal strength ($\|\boldsymbol{s}_1\|^2 = \|\boldsymbol{s}_2\|^2$).

3.2. ARL for the Special Case of Identical Sources

From (11) we can see that when $\boldsymbol{s}_1 = \alpha \boldsymbol{s}_2$, $\alpha \in \mathbb{R}\setminus\{0\}$, the first-order term vanishes and as a result (13) is inappropriate. Such a case should be considered separately. In this subsection, we focus on the case of two identical sources (i.e, $\boldsymbol{s}_1 = \boldsymbol{s}_2$). We assume that it is known to the detector that the two sources are identical under $\mathcal{H}_1$. It should be noted that a more practical problem would be without this assumption but is much more complicated. We have addressed it and the details will be given in a journal paper in preparation [19].

As it is reasonable to assume $\omega_0 = \omega_c$ according to (12), a second-order approximation of the signal model around ω_c gives

$$\boldsymbol{z} = \boldsymbol{A}\boldsymbol{x} + \boldsymbol{w} \tag{15}$$

with the definitions $\boldsymbol{x} \triangleq \boldsymbol{s}_1 + \boldsymbol{s}_2$, $\boldsymbol{A} \triangleq \boldsymbol{I}_L \otimes \boldsymbol{a}(\omega_c, \zeta)$, $\boldsymbol{a}(\omega_c, \zeta) \triangleq \boldsymbol{v}(\omega_c) + \zeta\ddot{\boldsymbol{v}}(\omega_c)$, $\zeta \triangleq \frac{\delta^2}{8}$ and $\ddot{\boldsymbol{v}}(\omega_c) \triangleq \frac{\partial^2 \boldsymbol{v}(\omega_c)}{\partial \omega_c^2}$. The binary hypothesis test formulation for the problem of resolution can be given by

$$\begin{cases} \mathcal{H}_0 \,:\, \zeta = 0,\ \boldsymbol{x} \\ \mathcal{H}_1 \,:\, \zeta > 0,\ \boldsymbol{x} \end{cases} \tag{16}$$

which is a one-sided test in the presence of nuisance parameters. The asymptotic PDF of the chi-squared distribution for the GLRT-based detector does not hold for this problem. Therefore, we resort to the Wald test instead and analyze its asymptotic statistical characteristics, as the Wald test and the GLRT were shown to have the same asymptotic performance for many problems [17]. Define the unknown parameter vector as $\boldsymbol{\xi} = [\boldsymbol{x}^T \quad \zeta]^T$. The Wald test for the problem in (16) can be computed by

$$T_w = \hat{\zeta}^2 \Big(\big[\boldsymbol{J}^{-1}(\hat{\boldsymbol{\xi}}_1)\big]_{\zeta\zeta} \Big)^{-1} \tag{17}$$

where $\hat{\zeta}$ is the constrained ($\hat{\zeta} \geq 0$) MLE of ζ under $\mathcal{H}_1$, $\hat{\boldsymbol{\xi}}_1$ is the MLE of $\boldsymbol{\xi}$ under $\mathcal{H}_1$, and $\big[\boldsymbol{J}^{-1}(\hat{\boldsymbol{\xi}}_1)\big]_{\zeta\zeta}$ is the value of the inverse of the Fisher information matrix corresponding to ζ calculated at $\hat{\boldsymbol{\xi}}_1$, i.e., the CRB of ζ calculated at $\hat{\boldsymbol{\xi}}_1$. Due to the known positivity of ζ, (17) can be rewritten by a one-sided Wald test

$$T_w = \hat{\zeta} \sqrt{\Big(\big[\boldsymbol{J}^{-1}(\hat{\boldsymbol{\xi}}_1)\big]_{\zeta\zeta} \Big)^{-1}} \tag{18}$$

The CRB of ζ can be calculated via the "complexified" approach [11] and is given by

$$\big[\boldsymbol{J}^{-1}(\boldsymbol{\xi})\big]_{\zeta\zeta} = \frac{\sigma^2}{2\|\boldsymbol{x}\|^2} \frac{N - 2\|\boldsymbol{d}\|^2\zeta + \|\boldsymbol{d} \odot \boldsymbol{d}\|^2\zeta^2}{N\|\boldsymbol{d} \odot \boldsymbol{d}\|^2 - \|\boldsymbol{d}\|^4} \tag{19}$$

Let $\hat{\zeta}_{\text{u}}$ denote the unconstrained MLE of ζ under $\mathcal{H}_1$. One can show that $\hat{\zeta}_{\text{u}}$ can be obtained by maximizing the quotient of two quadratic functions. We can prove that $\hat{\zeta}_{\text{u}}$ almost always exits, and $(\hat{\zeta}_{\text{u}})^+$ is a reasonable constrained MLE of ζ. Although the constrained MLE of ζ does not always exist, we can still use $(\hat{\zeta}_{\text{u}})^+$ as a sub-optimum choice. Due to the space limit, detailed explanation and the closed-form expression of $\hat{\zeta}_{\text{u}}$ will be given in [19].

Let $\eta_2 > 0$ denote the detection threshold. As $\Pr(\hat{\zeta} > \eta_2) = \Pr(\hat{\zeta}_{\text{u}} > \eta_2)$, following the derivation in [17, App. 6C], one can show that in the asymptotic sense, the detection performance of the Wald test-based detector can be characterized by

$$P_f = Q_{\mathcal{N}}(\eta_2) \tag{20}$$

$$P_d = Q_{\mathcal{N}}\Big(\eta_2 - \zeta\sqrt{\big([\boldsymbol{J}^{-1}(\boldsymbol{\xi}_0)]_{\zeta\zeta}\big)^{-1}}\Big) \tag{21}$$

where $Q_{\mathcal{N}}$ is the right-tail probability function for a standard Gaussian random variable (zero mean and unit variance), and $\boldsymbol{\xi}_0$ is the true value of $\boldsymbol{\xi}$ under $\mathcal{H}_0$. Finally, from (20) and (21) we obtain the ARL as

$$\delta^{(2)}_{\text{lim}} = 2\left(\frac{\sigma^2}{2\|\boldsymbol{s}_1\|^2} \frac{N\big(Q^{-1}_{\mathcal{N}}(P_f) - Q^{-1}_{\mathcal{N}}(P_d)\big)^2}{N\|\boldsymbol{d} \odot \boldsymbol{d}\|^2 - \|\boldsymbol{d}\|^4} \right)^{\frac{1}{4}} \tag{22}$$

where $Q^{-1}_{\mathcal{N}}$ is the inverse of $Q_{\mathcal{N}}$ and $\boldsymbol{s}_1$ can be replaced by $\boldsymbol{s}_2$ as $\boldsymbol{s}_1 = \boldsymbol{s}_2$.

4. SIMULATION RESULTS

In this section, we present some numerical examples to illustrate the validity of our analytical results on the ARLs derived in section III. The scenario is the following: the sensor array is a uniform linear array with $N = 10$ sensors and the inter-element spacing is $d = \frac{\nu}{2}$ (i.e., $d_i = \frac{\nu}{2}(-\frac{N+1}{2} + i), i = 1, \cdots, N$). The number of snapshots is $L = 100$. The prespecified probabilities of false alarm and detection are $p_f = 0.01$ and $p_d = 0.7$, respectively. The SNRs of the two sources are define as $\text{SNR}_1 = \frac{\|\boldsymbol{s}_1\|^2}{\sigma^2}$ and $\text{SNR}_2 = \frac{\|\boldsymbol{s}_2\|^2}{\sigma^2}$. The total SNR of the two sources is defined as $\text{SNR}_{\text{total}} = \frac{\|\boldsymbol{s}_1\|^2 + \|\boldsymbol{s}_2\|^2}{\sigma^2}$.

For fixed $\text{SNR}_{\text{total}} = 50$ dB in the case of two orthogonal sources ($\boldsymbol{s}_1^H \boldsymbol{s}_2 = \boldsymbol{s}_2^H \boldsymbol{s}_1 = 0$), we plot the SNR_1 versus $\delta_{\text{lim}}^{(1)}$ (in unit of $\frac{2}{\nu}$) for both the MPD criterion-based ARL and the ARL in [1, eqn. (55)] in Fig. 1. It is shown that the latter depends only on the total SNR, while the MPD criterion-based ARL coincides with it only when the two sources are of equal strength ($\text{SNR}_1 \approx 47$ dB) and increases as the difference of source strength increases.

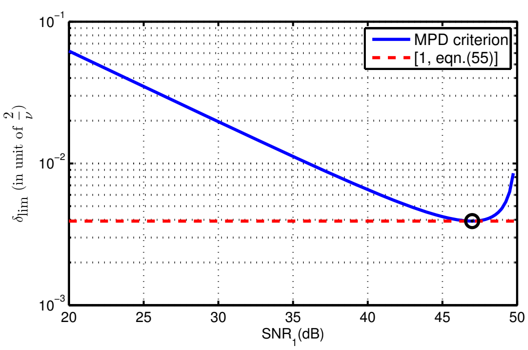

Fig. 1. SNR_1 versus $\delta_{\text{lim}}^{(1)}$ (in unit of $\frac{2}{\nu}$) with fixed $\text{SNR}_{\text{total}} = 80$ dB

A contour plot of (13) as a function of SNR_1 and SNR_2 in the case of two orthogonal sources is shown in Fig. 2. We observe that for a fixed SNR_1, the ARL decreases with SNR_2 increasing and converges to a fixed limit that can be derived from (13). (SNR_1 and SNR_2 are interchangeable here.)

The hypothesis test-based ARL given in (22) and the CRB criterion-based ARL in [11] are compared in Fig. 3 for the case of two identical sources. It can be seen that both ARLs have the same behaviour regarding the relation between the resolution limit and the total SNR: to increase the resolution tenfold, the total SNR must be increased by 40 dB for both methods.

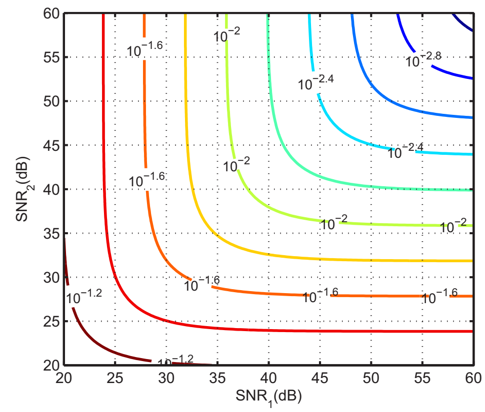

Fig. 2. Contour of $\delta_{\text{lim}}^{(1)}$ (in unit of $\frac{2}{\nu}$) as a function of SNR_1 and SNR_2

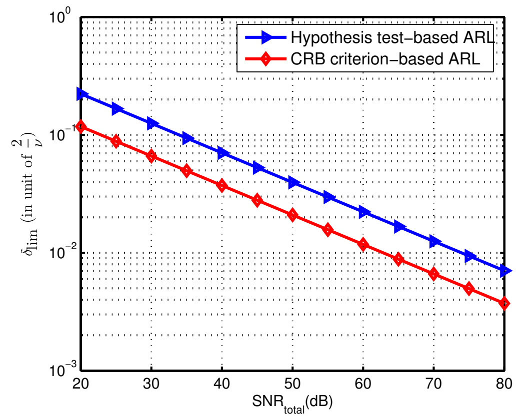

Fig. 3. ARL versus $\text{SNR}_{\text{total}}$

5. CONCLUSION

In this paper, we study the ARL of two closely-spaced sources in array processing based on the framework of hypothesis testing. A general linearized hypothesis test formulation is presented based on the first-order approximation of the signal model. Rather than assuming the parameter of the single source ω_0 to be the center parameter ω_c, we propose a criterion based on minimizing the probability of detection at a given probability of false alarm to determine ω_0. A new closed-form expression of the ARL for this general case is obtained by analyzing the worst case of the detection performance. Numerical examples verify the superiority of the proposed ARL over previous works.

We also investigate the special case of two identical sources where a second-order approximation is necessary. The hypothesis test in this case is a one-sided test in the presence of nuisance parameters. We resort to the Wald test and the corresponding ARL is derived by analyzing the asymptotic performance of the Wald test-based detector. Numerical simulations show that the derived ARL has the same behavior as the CRB criterion-based ARL with respect to the relation between the resolution limit and the total SNR.

6. REFERENCES

[1] M. N. El Korso, R. Boyer, A. Renaux, and S. Marcos, "On the asymptotic resolvability of two point sources in known subspace interference using a GLRT-based framework," *Signal Processing*, vol. 92, no. 10, pp. 2471–2483, Oct. 2012.

[2] M. N. El Korso, R. Boyer, A. Renaux, and S. Marcos, "Statistical resolution limit of the uniform linear cocentered orthogonal loop and dipole array," *Signal Processing, IEEE Transactions on*, vol. 59, no. 1, pp. 425 –431, Jan. 2011.

[3] M. N. El Korso, R. Boyer, A. Renaux, and S. Marcos, "Statistical resolution limit for source localization with clutter interference in a MIMO radar context," *Signal Processing, IEEE Transactions on*, vol. 60, no. 2, pp. 987 –992, Feb. 2012.

[4] N. D. Tran, R. Boyer, S. Marcos, and P. Larzabal, "Angular resolution limit for array processing: Estimation and information theory approaches," in *Signal Processing Conference (EUSIPCO), 2012 Proceedings of the 20th European*, Aug. 2012, pp. 101 –105.

[5] Q. T. Zhang, "Probability of resolution of the MUSIC algorithm," *Signal Processing, IEEE Transactions on*, vol. 43, no. 4, pp. 978 –987, Apr. 1995.

[6] M. Kaveh and A. Barabell, "The statistical performance of the MUSIC and the minimum-norm algorithms in resolving plane waves in noise," *Acoustics, Speech and Signal Processing, IEEE Transactions on*, vol. 34, no. 2, pp. 331 – 341, Apr. 1986.

[7] A. Ferreol, P. Larzabal, and M. Viberg, "Statistical analysis of the MUSIC algorithm in the presence of modeling errors, taking into account the resolution probability," *Signal Processing, IEEE Transactions on*, vol. 58, no. 8, pp. 4156–4166, Aug. 2010.

[8] H. S. Mir and J. D. Wilkinson, "Radar target resolution probability in a noise-limited environment," *Aerospace and Electronic Systems, IEEE Transactions on*, vol. 44, no. 3, pp. 1234 –1239, Jul. 2008.

[9] H. S. Mir and B. D. Carlson, "Range resolution of unequal strength targets," in *Radar Conference - Surveillance for a Safer World, 2009. RADAR. International*, Oct. 2009, pp. 1 –5.

[10] H. B. Lee, "The Cramér-Rao bound on frequency estimates of signals closely spaced in frequency," *Signal Processing, IEEE Transactions on*, vol. 40, no. 6, pp. 1507 –1517, Jun. 1992.

[11] S. T. Smith, "Statistical resolution limits and the complexified Cramér-Rao bound," *Signal Processing, IEEE Transactions on*, vol. 53, no. 5, pp. 1597 – 1609, May. 2005.

[12] M. Shahram and P. Milanfar, "On the resolvability of sinusoids with nearby frequencies in the presence of noise," *Signal Processing, IEEE Transactions on*, vol. 53, no. 7, pp. 2579 – 2588, Jul. 2005.

[13] M. Shahram and P. Milanfar, "Statistical and information-theoretic analysis of resolution in imaging," *Information Theory, IEEE Transactions on*, vol. 52, no. 8, pp. 3411 –3437, Aug. 2006.

[14] Z. Liu and A. Nehorai, "Statistical angular resolution limit for point sources," *Signal Processing, IEEE Transactions on*, vol. 55, no. 11, pp. 5521 –5527, Nov. 2007.

[15] A. Amar and A. J. Weiss, "Fundamental limitations on the resolution of deterministic signals," *Signal Processing, IEEE Transactions on*, vol. 56, no. 11, pp. 5309 –5318, Nov. 2008.

[16] P. Stoica, V. Simonytė, and T. Söderström, "On the resolution performance of spectral analysis," *Signal Processing*, vol. 44, no. 2, pp. 153–161, Jan. 1995.

[17] S. M. Kay, *Fundamentals of Statistical Signal Processing: Detection Theory*, vol. 2, NJ: Prentice Hall, 1998.

[18] A. Renaux, P. Forster, E. Chaumette, and P. Larzabal, "On the high-SNR conditional maximum-likelihood estimator full statistical characterization," *Signal Processing, IEEE Transactions on*, vol. 54, no. 12, pp. 4840–4843, Dec. 2006.

[19] W. Zhu, S. Wan, and J. Tang, "Angular resolution limit of two closely-spaced point sources based on hypothesis testing," *in preparation*.